WIPL-D Pro v16: What is New in Numerical Engine?

New features/improvements introduced in v16 are:

1. **Periodic Boundary Condition (PBC):**
   a. **2D periodic structure**
   b. **Plane wave illumination**
   c. **3D cell in a form of arbitrary composite material structure**
   d. **Complex connections at boundaries of neighboring cells**
   e. **FSS, Meta & Nano materials, Diffraction grating, Absorber & Reflect arrays**
2. **ULTRA higher order bases**
   a. **Maximum expansion order increased from 8 to 32**
   b. **Maximum patch size enlarged from 2 λ to 10 λ**
   c. **Increased efficiency and accuracy for complex and large structures**
   d. **Advanced convergence tests based on p-refinement**
3. **New Edging technique - "Refined" edging**
   a. **Efficiency of "Classic", but robustness of "Advanced" edging**
4. **GPU Cluster Solver:**
   a. **Support for arbitrary number of GPUs per node with improved efficiency**
5. **Other options/improvements:**
   a. **Determining required number of unknowns**
   b. **Avoided with Interpolation available now in Remote Run mode**
   c. **Custom defined excitation waves and radiation directions for RCS**

1. Periodic Boundary Condition (PBC)

PBC works with 2D periodic scatterers.

a) 2D periodic structure: the problem description

A 2D periodic structure consists of identical 3D objects periodically repeated in the *xOy*-plane. The periods along *x*- and *y*-axis are d_x and d_y, respectively.

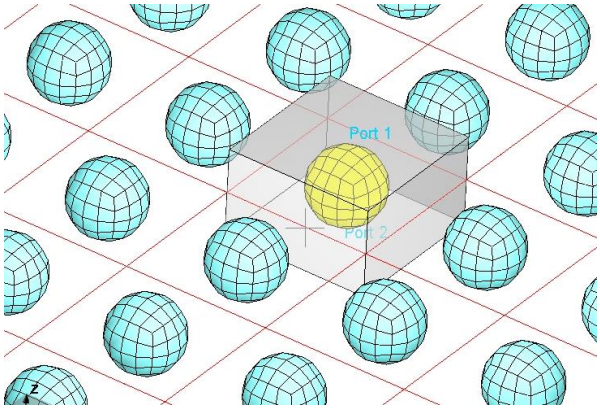

Fig. 1. Sketch of 2D periodic structure

The border of a cell is specified by its *x*, *y*, and *z*-coordinate, x_1, x_2, y_1, y_2, z_1, and z_2, so that $d_x = x_2 - x_1$, $d_y = y_2 - y_1$, and $z_1 < z < z_2$. The boundary surfaces of the cell at $z = z_2$ and $z = z_1$ represent Port 1 and Port 2 of the cell, respectively. The space above Port 1 is filled by vacuum (Domain 1), while the space below Port 2 can be filled by arbitrary material including vacuum (Domain 1, Domain 2, etc.).

b) Plane wave illumination: the problem solution

The structure is excited from above, i.e., through the Port 1, by a TEM plane wave of arbitrary polarization and incoming direction $(0° < \theta \leq 90°)$. Reflected waves from Port 1 and transmitted waves through Port 2 are TEM plane waves and TE and TM Floquet waves (modes).

By default, the simulation yields solution for electric currents along the PEC wires and over the PEC plates, and equivalent electric and magnetic currents over dielectric surfaces, inside the unit cell.

The *s*-parameters of these waves, $s_{\phi 11}$, $s_{\theta 11}$, $s_{\phi 21}$, and $s_{\theta 21}$, are calculated with respect to incident wave of arbitrary polarization: The first numerical index in these definitions represents the port at which the response is inspected, and the second index represents the port that is excited by the plane wave. The phases of all waves are related to the coordinate origin.

Obtained complex powers are normalized by the power of the TEM plane wave incident at Port 1, resulting in complex power reflection and transmission coefficients, p_{11} and p_{21}. Real parts of p_{11} and p_{21} are related to propagating TEM and Floquet modes. The imaginary parts are related to evanescent Floquet modes.

In addition to default calculation the user can opt to calculate: a) the current distributions along/over the wires/plates inside the cell, b) the near field distribution in arbitrary grid of points in the space, and c) the radiation pattern due to unit cell.

The near field distribution inside the cell ($z_1 < z < z_2$) and their periodic copies is specified and calculated in the same way as for non-periodic structures. Above the cells ($z > z_2$) only the scattered near field is calculated, while below ($z < z_2$) only the transmitted field is calculated.

The EM object inside a cell is an arbitrary composite metallic and dielectric structure. The cells can be connected in arbitrary ways through their common faces by using the PEC and/or the material bodies.

c) FSS, Meta/Nano materials, Diffraction grating, Absorber/Reflect arrays

The feature offers **field/power reflection/transmission coefficients** (R/T), as well as corresponding **near/far field distribution**. A number of examples is a part of setup: **boundary surface vacuum/dielectric** (validates Snell law and agrees with analytical formula), **cross and cross aperture** (complementary behavior), **Jerusalem cross** (excellent agreement with literature), **slot apertures in PEC screen** (the skewed lattice can be arranged as orthogonal lattice), **strip-mesh PEC screen** (in two variants, window and cross, with the same results), **dielectric EBG structure** (excellent agreement with literature).

Example:

Let us consider the pyramidal absorber (Fig. 2a). The base of absorber, which coincides with the base of the unit cell is square of side $a = 5$ mm.

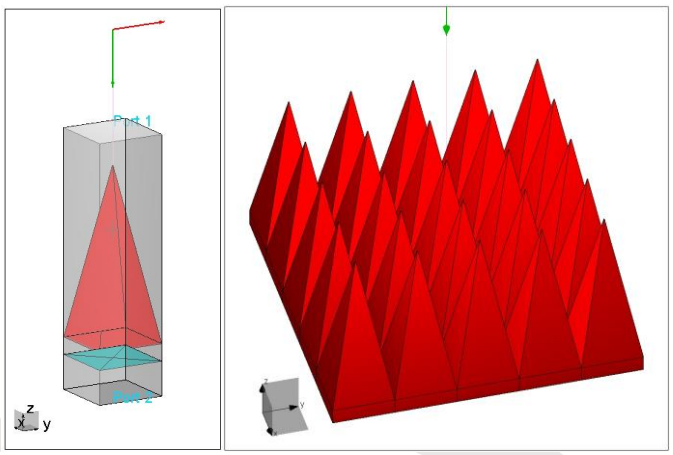

a) unit cell b) finite array of absorbers

Fig. 2. Pyramidal absorber

The height of the pyramid is $h = 2.5a$. The pyramid is placed on pedestal of the same base of height $d = a/4$. The absorber is made of material whose relative electric constant and conductivity are $\varepsilon_r = 1.3$ and $\sigma = 10$ S/m. The bottom of pedestal, which is place in *xOy*-plane, is covered by PEC infinitesimally thin plate. Fig. 3 shows the reflection coefficient (in dB) in range from 10 GHz to 60 GHz. Fig. 4 shows near field distribution in *yOz*-plane inside the unit cell at one moment in time at frequency of 50 GHz. Electric field is shown in Fig. 4a, and magnetic field is shown in Fig. 4b.

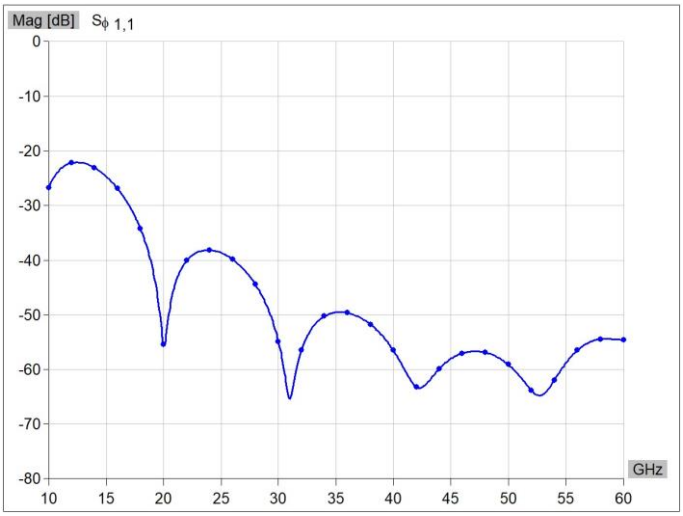

Fig. 3. Reflection coefficient versus frequency for pyramidal absorber from Fig. 2.

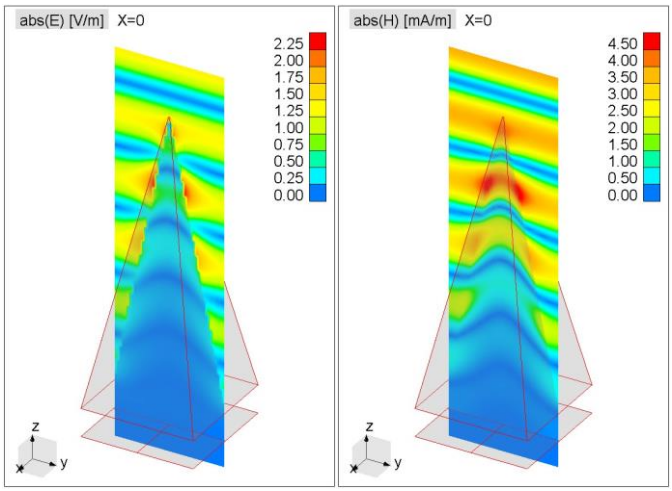

a) electric field b) magnetic field

Fig. 4. Near field distribution in xOz-plane inside the unit cell in one moment of time.

2. ULTRA higher order bases

This release introduces max-ortho (orthogonal) bases implemented using decomposition into Legendre polynomials. This results in extreme stability/accuracy and

extends the limits to d_{max} = 10 λ for maximum patch size and n_{max} = 32 for maximum expansion order. Thus, new bases will be referred to as ULTRA higher order basis functions (ULTRA HOBFs).

ULTRA higher order bases enable user to:

1. improve the simulation efficiency (reduce number of unknowns for electrically large structures),
2. improve accuracy of the results (by *p*-refinement),
3. perform advanced convergence tests, and
4. increase the confidence in the obtained results without the comparison to other software or measurement.

Example:

Let us consider model of airplane fighter, 12 m long, as shown in Fig. 5. The plane is illuminated by θ-polarized plane wave incoming from direction ϕ = 0°, θ° = -30°. At frequency of *f* = 2.5 GHz, the total electric length of the airplane is D = 100 λ. The half of the model is constructed using 103 quadrilateral plates, whose minimum and maximum edge lengths are 0.05 λ and 25 λ, respectively. The result of simulation is bistatic RCS in *xOz*-plane, the vertical symmetry plane for the fuselage. This symmetry plane halves the number of unknowns.

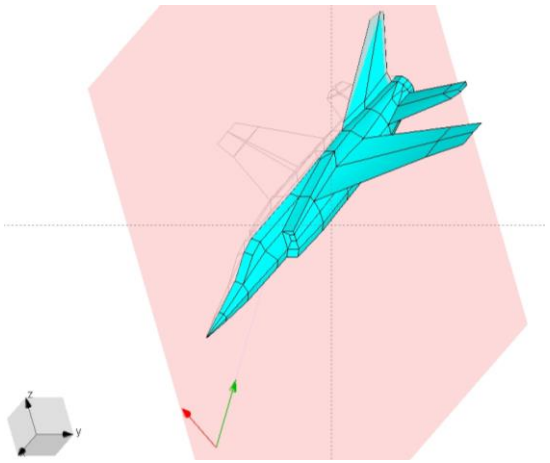

Fig. 5. Aircraft illuminated by a plane wave

In the fist step, the simulation is performed using various values of maximum patch size, i.e. $d_{max} = k\,\lambda$, k = 1/10, 1/3, 1, 2, 3, … 9, 10. In order to achieve high precision of evaluation of matrix equation elements the integral accuracy is set to Enhanced 2 for $k \le 4$, Enhanced 3 for $4 < k \le 7$, and Enhanced 4 for $7 < k \le 10$, while all other simulation parameters are set to default values. Thus, the plates, whose length is greater than d_{max}, will be automatically subdivided into minimum number of plates not longer than d_{max}. For each maximum patch size Table 1 shows the maximum expansion order and total number of unknowns N_0. It is seen that by increasing the maximum patch size the number of unknowns decreases quickly up to d_{max} = 3 λ, and then slowly up to d_{max} = 6 λ. Such behavior is explained by the fact that most of the plates has maximum dimension between 3 λ and 6 λ.

Table 1. For aircraft 12m long shown in Fig. 5 and simulated at 2.5 GHz, maximum order and numbers of unknowns N_0, N_1, and N_2, are given for various maximum patch sizes.

Maximum Patch Size	*Maximum Order n*	N_0	N_1	N_2
0.1 λ	1	938,052	-	-
0.33 λ	2	234,513		
1 λ	4	104,996		
2 λ	7	86.651	118,829	157,423
3 λ	10	76,122	97,650	121,866
4 λ	13	75,554	93,092	112,492
5 λ	16	75,321	90,705	107,533
6 λ	19	74,376	88,668	104,248
7 λ	22	76,960	90,364	104,868
8 λ	25	78,035	90,805	104,563
9 λ	28	79,078	91,638	105,138
10 λ	31	78,858	90,885	103,692

Fig. 6 shows RCS in xOz-plane for various values of maximum patch size. It is seen that all results practically coincide. Small numerical noise can be observed at levels 50 dB below the main lobe.

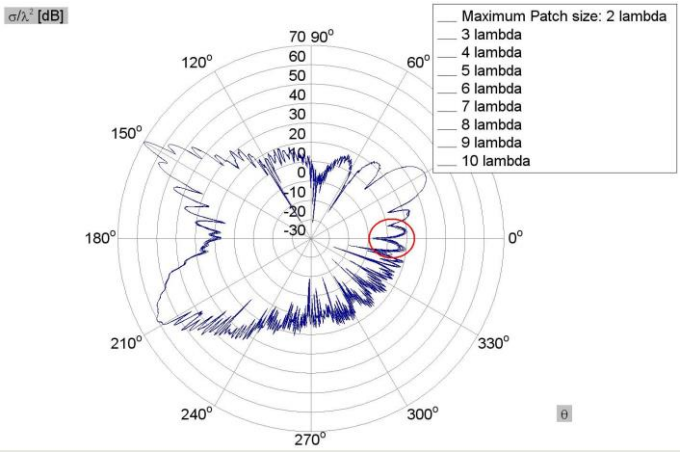

Fig. 6. RCS for various maximum patch sizes

For example, let's focus on the expanded view of the encircled part of the graph from Fig. 6, which is shown in Fig. 7. In this specific range, the spread of the results is between 2 dB and 10 dB.

The accuracy of the results can be improved in numerous ways. The two basic are: 1) increasing the reference frequency, and 2) increasing the expansion order by 1, or even 2 (used here).

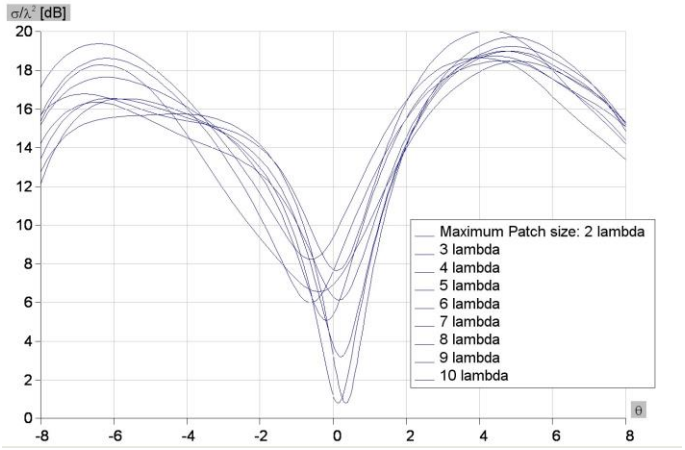

Fig. 7. Detail of RCS results in xOy-plane (encircled in Fig. 6)

Increase of the order by 1 or by 2 increases the total number of unknowns from N_0 to N_1 and N_2. The increased numbers of unknowns are also shown in Table 1. It is seen that by increasing the maximum patch size the number of unknowns decreases relatively quickly up to d_{max} = 10 λ.

Figs. 8 and 9 show the same results as Figs. 6 and 7, but obtained by using the expansion order increased by 1 (i.e. using N_1 unknowns instead of N_0 unknowns.) It is seen that numerical noise is significantly reduced. In particular, it is seen in Fig. 9 that in this specific range the spread of the results is from 0.5 dB to 2 dB.

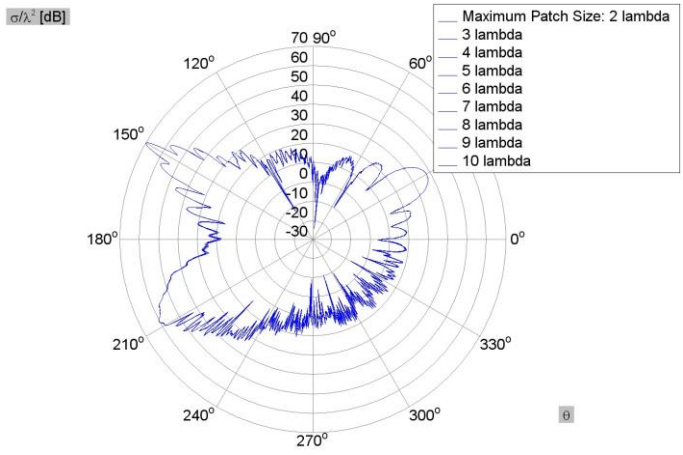

Fig. 8. RCS for various maximum patch sizes. The same results as shown in Fig. 6, but using expansion order increased by 1 (N_1 unknowns)

Finally, in the 3rd step let us consider the case when the aircraft is simulated at 7.5 GHz. The corresponding numbers of unknowns, N_0, N_1, and N_2, are given in Table 2. Since the most of the plates are of the maximum size of 10 λ, or greater, a continuous decrease of a number of unknowns is observed for increase of maximum patch size up to 10 λ even for N_0.

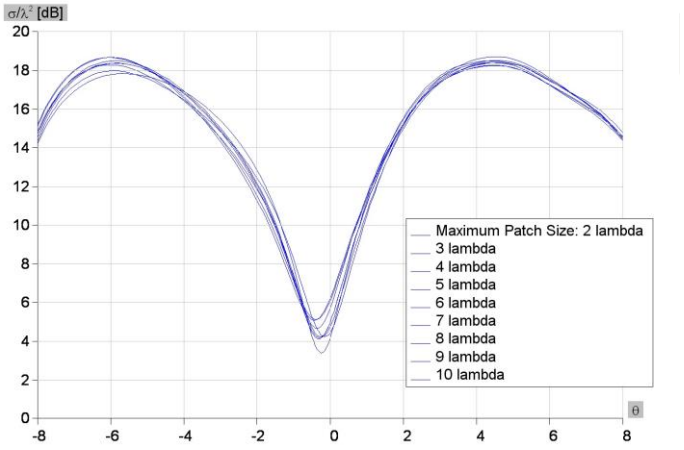

Fig. 9. The same results as shown in Fig. 7, but using expansion order increased by 1 (N_1 unknowns)

Table 2. For aircraft 12m long shown in Fig. 5 and simulated at 7.5 GHz, maximum order and numbers of unknowns N_0, N_1, and N_2, are given for various maximum patch sizes.

Maximum Patch Size	*Maximum Order*	N_0	N_1	N_2
2 λ	7	662,747	886,637	1,142,983
3 λ	10	606,386	753,446	916,418
4 λ	13	590,300	702,448	824,341
5 λ	16	590,231	683,719	784,071
6 λ	19	604,493	687,913	776,749
7 λ	22	588,216	658,033	731,790
8 λ	25	582,117	644,427	709,913
9 λ	28	573,974	630,586	689,886
10 λ	31	564,909	616,354	667,853

Conclusion:

ULTRA higher order bases are recommended for advanced use, such as reducing the number of unknowns for electrically large structures. Theoretically, using 10 λ instead of 2 λ for maximum patch size for default simulations, the maximum reduction is 22% in number of unknowns and 55% in simulation time. However, depending on the size of the problem, the optimal maximum patch size can be anywhere between 2 λ and 10 λ. The average reduction is around 15% in number of unknowns and 40% in matrix solution time.

They can be also used to perform advanced convergence tests in efficient way based on controllable increase of the expansion order.

In particular, such advanced convergence tests enable, if required, obtaining the results with extremely high precision. Such high precision results can be used either as unique benchmarks for other solutions, or to build confidence in the results without comparing them with other software or measurement.

3. "Refined" Edging Technique

The feature takes into the account the edge effects more accurately by an additional meshing along critical edges. There were two types of edging in the previous WIPL-D Pro release: 1) "classic", and 2) "advanced". The new version introduces the third type of "edging", under the name "refined". The "refined" combines efficiency of "classic" and robustness of "advanced".

Example:

Let us consider PCB with two infinitesimally thin metallic patches placed at top surface of substrate (Fig. 10).

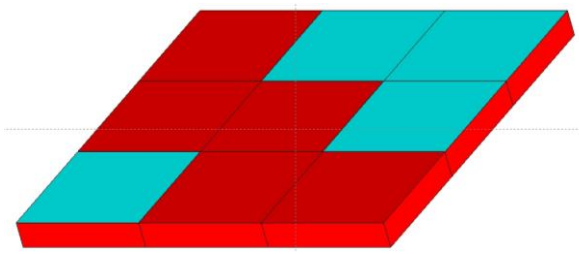

Fig. 10. Model of PCB: two simple infinitesimally thin metallic patches are placed at top surface of substrate.

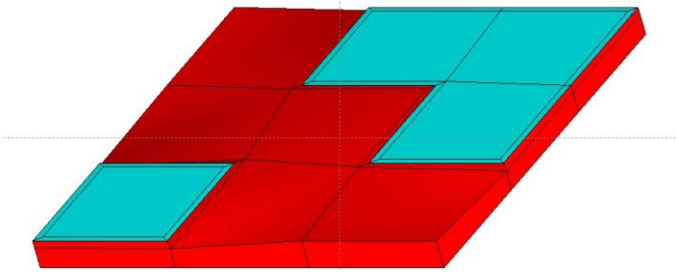

a) "classic"

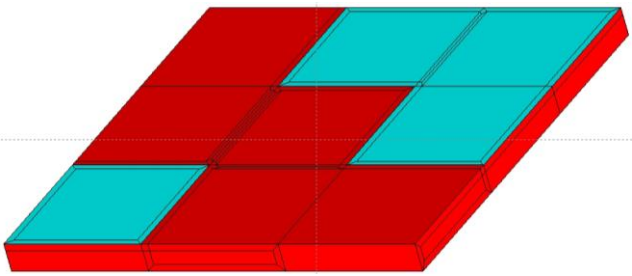

b) "advanced"

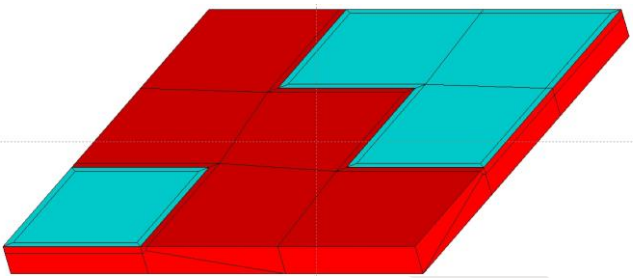

c) "refined"

Fig. 11. Model of PCB obtained after edging

After applying 3 types of edging the corresponding geometrical models are shown in Fig. 11. It is seen that "classic" results in relatively rough model, while "advanced" and "refined" completely preserve the original shape.

The number of plates and unknowns after edging is given in Table 3.

Table 3. Number of plates and unknowns after applying 3 types of edging to PCB shown in Fig. 10.

Number of	*Classic*	*Advanced*	*Refined*
Plates	70	110	78
Unknowns	552	760	624

4. GPU Cluster Solver:

Usage of an arbitrary number of GPUs per compute node is supported in the new version of GPU Cluster Solver. Multi-node and multi-GPU parallelization efficiencies are significantly improved when compared with previous versions of the GPU Cluster Solver.

5. Other options/improvements:

a) Determining required number of unknowns

Invoking the feature checks the required number of unknowns in hand, before the EM simulation is started.

b) Avoided with Interpolation available now in Remote Run mode

The Avoided with Interpolation simulations is now available in Remote Run mode. From user's point of view, usage of the option is exactly the same as in regular run on local machine, the only difference is the fact that Run Localization is set to Remote.

c) Custom defined excitation waves and radiation directions for RCS

In addition to NWA file introduced in v15, NWB file was introduced in v16. While NWA file allows a user to define uniform grid of angles of the RCS response for each excitation wave, NWB file allows definitions of non uniform grid for both, excitation waves and RCS directions.